RESEARCHERID
THOMSON REUTERS

[Silva* *et al.*, 7(6): June, 2018]
IC™ Value: 3.00

ISSN: 2277-9655
Impact Factor: 5.164
CODEN: IJESS7

IJESRT

INTERNATIONAL JOURNAL OF ENGINEERING SCIENCES & RESEARCH TECHNOLOGY

# NUMERICAL ANALYSIS IN FINITE ELEMENTS OF LAMINATED PLATES IN STEEL APPLIED IN DIFFERENT TYPES OF COMPOSITE MATERIALS MODELED ABAQUS MODELING AND COMPARED WITH ANALYTICAL

**Welington Vital da Silva[*1], Brunno Emidio Sobrinho[1], Cleirton André Silva Freitas[2],**

**Brenda A. Távora Ribeiro[3], Francisco F. S. de Morais Júnior[3], Ramon S. Y. R. Costa Silva [4]**

[*1] Doctorate in Structures, Department of Civil Engineering, University of Brasília – UnB. Asa Norte, Campus Darcy Ribeiro, Brasilia, DF, Brazil

[2] Professor PhD in Civil Engineering, UFCA – Federal University of Cariri, Av. Lieutenant Raimundo Rocha S/N and University City of Juazeiro do Norte, Ceará, CE, Brazil

[3] Civil engineering student, UFCA – Federal University of Cariri, Av. Lieutenant Raimundo Rocha S/N and University City of Juazeiro do Norte, Ceará, CE, Brazil

[4] Doctor in Structures, Department of Civil Engineering, University of Brasília – UnB. Asa Norte, Campus Darcy Ribeiro, Brasilia, DF, Brazil

**DOI**: 10.5281/zenodo.1299053

## ABSTRACT

The structures formed by laminated composites have great application in civil engineering. Mainly covering of industries with trapezoidal tile with acoustic insulation. Another application of the composite system is in the green layers of the roof. So this paper discussed a formulation for stability analysis of laminated plates through the Finite Element Method. The formulation presented allows the use of triangular and quadrilateral elements with different interpolation orders. In the numerical examples, the quadratic finite element with quadratic interpolation C3D8R was used to study its behavior. The reduced integration technique was used to alleviate the shear block problem. The behavior of these elements was evaluated by comparing the results obtained by FEM with analytical solutions based on the classical laminated plate theory. The results show that the elements provided excellent precision results for cross-layer laminates and single and biaxial angles and loads.

**KEYWORDS**: Laminated Plates, Finite Elements, Non Geometric Linearity and ABAQUS

## I. INTRODUCTION

In the design of structures, linear models are usually used for stress analysis. However, linear analysis is valid only when the structure suffers just small deformations and displacements and its material has linear elastic behavior, obeying Hooke's Law. When the displacements and deformations increase or the behavior of the material presents phenomena such as plasticity and cracking, the nonlinear effects gain importance.

In the general case, both geometric nonlinearity due to large displacements and physical non-linearity due to material's mechanical behavior need to be considered. However, slender structures may lose stability without sufficient applied loads to cause material degradation. Thus, in the study of the stability of these structural elements it can be assumed that the material remains in the linear elastic regime and the loss of stability is caused only by geometric non-linearity.

Plate stability analysis involves the solution of partial differential equations (Reddy, 1996). Even in the case of homogeneous and isotropic plates, these equations only have exact (closed) solutions for simple geometries, loads and boundary conditions. In order to eliminate this limitation and allow the solution of practical cases, the Finite Element Method (FEM) was used.

ISSN: 2277-9655
Impact Factor: 5.164
CODEN: IJESS7

The focus of this paper will be the stability analysis of laminated plates using FEM. It will be used finite elements based on the first order shear deformation theory, also known as Reissner-Mindlin's plate theory (Reddy, 1996; Bathe, 1996; Cook et al., 2002) and the non-linear effects will be taken into account through the use of von Kármán's theory (Crisfield, 1991). Particularly, it will be studied the behavior of a quadratic quadrilateral element of eight knots C3D8R in ABAQUS.

The formulation presented here was implemented in the Matlab software, which is a free software for structural analysis through Finite Element Method that uses the philosophy of Object Oriented Programming. The numerical results will be compared with the analytical solution of some classic problems found in the literature (benchmarks) in order to validate the proposed formulation and implementation.

## II. MATERIALS AND METHODS

### *1. Composite materials*

Composite materials are formed by two or more materials combined on a macroscopic scale, aiming to obtain a material with desired properties not obtained in the individual components (Reddy, 1996). Composite materials are generally classified in three different types: particulate composites, fibrous composites or laminated composites (Jones, 1999), as shown in Figure 1.

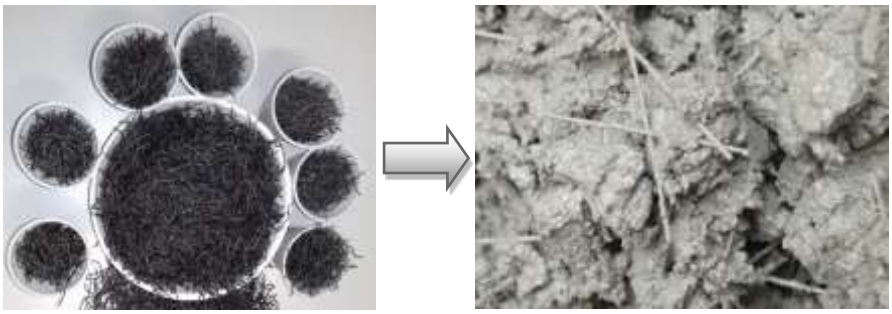

***A) Composite material with fiber: Concrete with steel fiber***

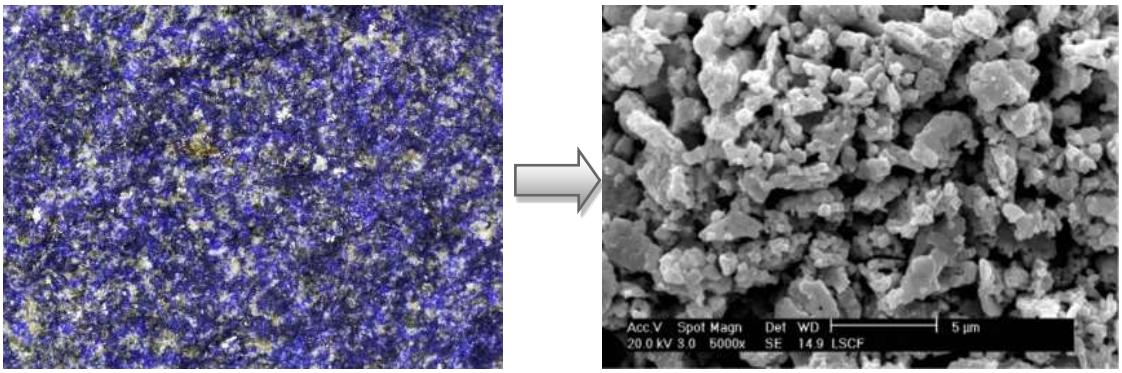


***B) Composite formed by particles: Rocks formed by crystals***

***(C)Types of composites used in industrial roofing***

ISSN: 2277-9655
Impact Factor: 5.164
CODEN: IJESS7

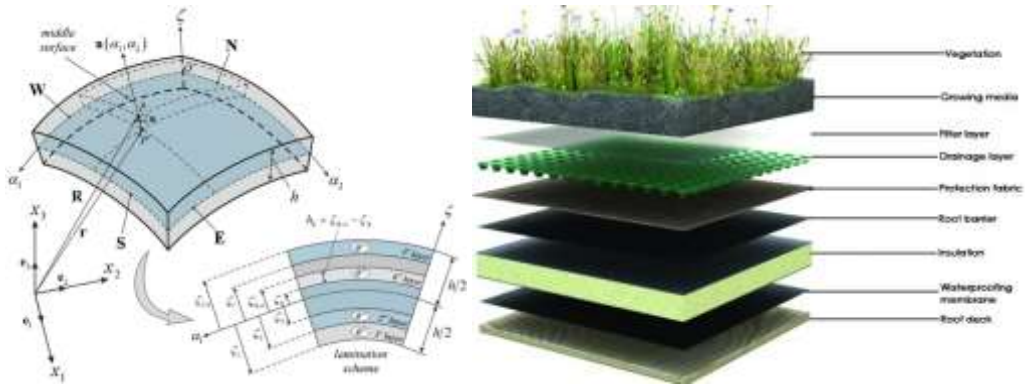


**(D)** ***Laminated Composite***

**Figure 1** - ***Different types of composite materials***

The structural members fabricated using laminated composites are formed by a series of layers joined to work in solidarity. A common example of a composite obtained in this way is plywood. However, for the fabrication of high performance structural elements, the most widely used materials are fiber reinforced composites (Jones, 1999; Reddy, 1996). In this case, each blade is formed by a set of fibers of high strength and stiffness embedded in the base material or matrix of lower strength and stiffness, but mainly of lower cost. In this way, each layer behaves macroscopically as an orthotropic material, whose main directions are parallel and perpendicular to the fibers.

## *2. Laminated Composite*

The structures formed by laminated composites have great application in civil engineering. Mainly covering of industries with trapezoidal tile with acoustic insulation. Another application of the composite system is in the green layers of the roof.

Green roofs offer a variety of benefits for the resident and the city, including reduced energy costs, extended roof life, rainwater retention and improved air quality.

Several incentives to use this system are being implemented in Europe and the United States, led by nonprofit philanthropic organizations. One is the Anacostia Watershed Society, a non-profit organization that facilitates the Green Roof Rebate program of the District Energy Department, which covers a certain cost per square foot of its green roof.

In this way, the layer represents the fundamental block of laminated composites (Reddy, 1996). The layers have high strength and modulus of elasticity in the direction of the fibers and low values in the orthogonal direction to the fibers. The laminated composites are constructed according to a layer structure, which is defined by the number of layers, orientation of the fibers (θ) and thickness of each layer, as shown in Figure 2.

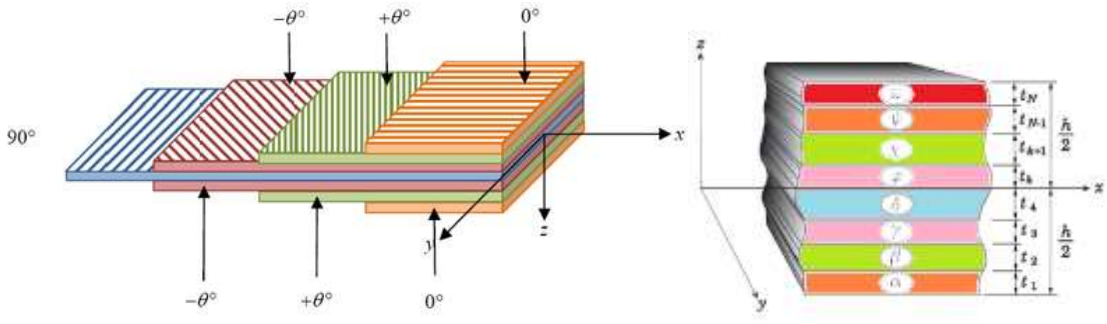


**Figure 2** - ***Several layers of the composite material on the reference axis***

ISSN: 2277-9655
Impact Factor: 5.164
CODEN: IJESS7

Due to the orthotropic characteristic of each layer, the composites can be fabricated in such a way as to obtain a maximum advantage in each specific situation by placing the direction of the fibers along the most requested directions (path of the loads). In this way, it can be obtained from highly optimized projects by changing the number, thickness, and sequence of the layers, as well as the orientation of the fibers of each layer.

### *3. Constitutive conditions*

Laminated composites are formed by several layers and each one has fibers oriented in different directions. Then, the analysis of laminated structures requires the use of a global coordinate system (x, y, z) in which the differential equations of equilibrium and kinematic conditions are written, while the constitutive conditions of the material are written in the local coordinate system or of the material ($x_1$, $x_2$, $x_3$), As shown in Figure 3.

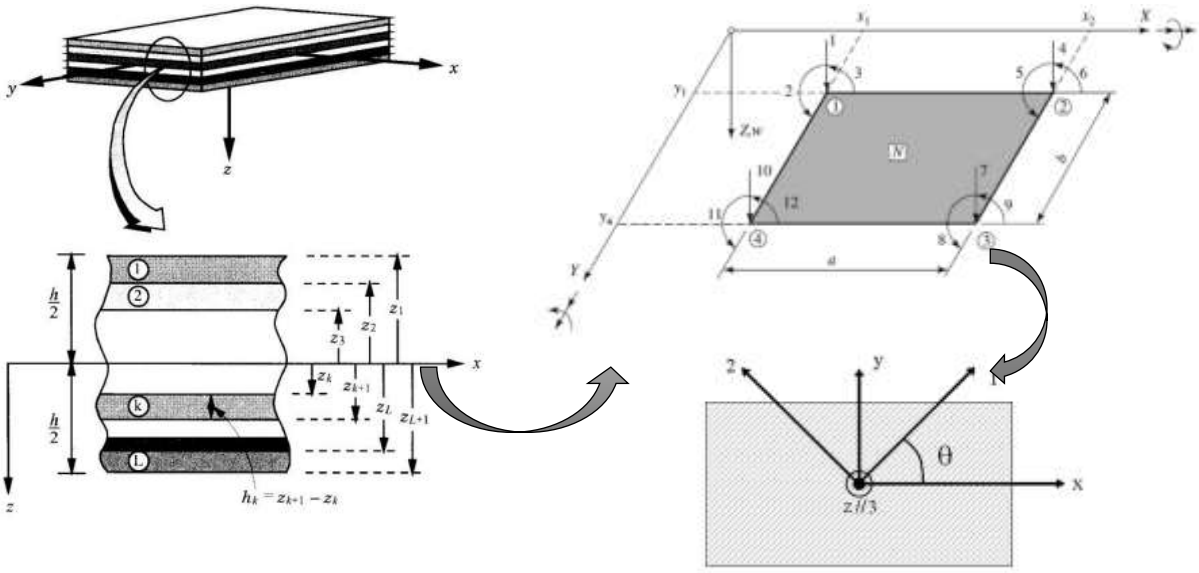


**Figure 3** - ***Layers of a laminate. Reddy (2004)***

In layers with unidirectional fibers, the x1 axis is oriented parallel to the fibers, making an angle θ with the principal axis x. The x2 axis is perpendicular to the fibers in the plane of the plate and the x3 axis is perpendicular to the plane of the plate, as shown in Figure 3. Since the material of each layer is considered homogeneous and orthotropic, it is necessary to establish a relation between the coordinate system of the plate material (x1, x2, x3) and the global coordinate system (x, y, z).

It is verified experimentally (Jones, 1999) that in usual service conditions the mechanical behavior of the layers can be considered as elastic linear, using the Hooke's Law generalized to represent the stress-strain relationship. For orthotropic materials the stress-strain relationship in each layer is given by.

$$\boldsymbol{\sigma} = \mathbf{C}\,\boldsymbol{\varepsilon} \tag{1}$$

Where **C** is the elastic constitutive matrix.

$$\mathbf{C}_{ijkl} = \lambda\delta_{ij}\delta_{kl} + \mu(\delta_{ik}\delta_{jl} + \delta_{il}\delta_{jk}) \tag{1a}$$

Where λ and μ are the Lamé constants. The constant μ is equivalent to the transversal modulus of elasticity, that is, μ ≡ G = E 2 (1 + ν). On the other hand, the constant λ relates to the longitudinal modulus of elasticity E and the Poisson coefficient ν through the following expression λ = νE (1 + ν) (1-2ν).

Therefore, the strain versus strain ratio is given by: $\sigma_{ij} = \mathbf{C}_{ijkl}\varepsilon_{kl}$ .

In practice, this matrix is obtained by inverting the stress-strain relationship:

ISSN: 2277-9655
Impact Factor: 5.164
CODEN: IJESS7

$$\begin{Bmatrix}\varepsilon_1\\ \varepsilon_2\\ \varepsilon_3\\ \gamma_{23}\\ \gamma_{13}\\ \gamma_{12}\end{Bmatrix}=\begin{bmatrix}S_{11} & S_{12} & S_{13} & 0 & 0 & 0\\ S_{12} & S_{22} & S_{23} & 0 & 0 & 0\\ S_{13} & S_{23} & S_{33} & 0 & 0 & 0\\ 0 & 0 & 0 & S_{44} & 0 & 0\\ 0 & 0 & 0 & 0 & S_{55} & 0\\ 0 & 0 & 0 & 0 & 0 & S_{66}\end{bmatrix}\begin{Bmatrix}\sigma_1\\ \sigma_2\\ \sigma_3\\ \tau_{23}\\ \tau_{13}\\ \tau_{12}\end{Bmatrix} \Rightarrow \boldsymbol{\varepsilon}_1 = \mathbf{S}\boldsymbol{\sigma}_1 . \quad (2)$$

In this equation **S** is the matrix of flexibility (or compliance) of the material, whose coefficients are given by:

$$S_{11}=\frac{1}{E_1};\ S_{12}=\frac{-\upsilon_{21}}{E_2}=\frac{-\upsilon_{12}}{E_1};\ S_{13}=\frac{-\upsilon_{31}}{E_3}=\frac{-\upsilon_{13}}{E_1};\ S_{22}=\frac{1}{E_2};$$
$$S_{23}=\frac{-\upsilon_{32}}{E_3}=\frac{-\upsilon_{23}}{E_2};\ S_{33}=\frac{1}{E_3};\ S_{44}=\frac{1}{G_{23}};\ S_{55}=\frac{1}{G_{31}};\ S_{66}=\frac{1}{G_{12}} \quad (3)$$

Where $E_1$, $E_2$ and $E_3$ are the moduli of elasticity in the principal directions, $v_{12}$, $v_{21}$, $v_{13}$, $v_{31}$, $v_{23}$, $v_{32}$ are the Poisson coefficients and $G_{12}$, $G_{13}$ e $G_{23}$ are the shear moduli of elasticity. It is important to note that orthotropic elastic materials have only 9 independent constants, since the Poisson coefficients ( $\upsilon_{ij}$ ) must satisfy the relation:

$$\frac{\upsilon_{ij}}{E_i}=\frac{\upsilon_{ji}}{E_j} \qquad (i,\ j=1,2,3), \quad (4)$$

Since the **S** matrix is symmetric.

The relation between the coordinates of the material ($x_1$, $x_2$, $x_3$) and the global reference system ($x$, $y$, $z$) is defined from the orientation of the fibers ($\theta$) with respect to the x-axis of the global system, as shown in Figure 3. The change of coordinate system is performed through the transformation:

$$\begin{Bmatrix}x_1\\ x_2\\ x_3\end{Bmatrix}=\begin{bmatrix}\cos\theta & sen\theta & 0\\ -sen\theta & \cos\theta & 0\\ 0 & 0 & 1\end{bmatrix}\begin{Bmatrix}x\\ y\\ z\end{Bmatrix} \Rightarrow \mathbf{x}_1 = \mathbf{A}\,\mathbf{x} . \quad (5)$$

The transformation of the $u_1, u_2$ and $u_3$ displacements is carried out in an analogous way:

$$\begin{Bmatrix}u_1\\ u_2\\ u_3\end{Bmatrix}=\begin{bmatrix}\cos\theta & sen\theta & 0\\ -sen\theta & \cos\theta & 0\\ 0 & 0 & 1\end{bmatrix}\begin{Bmatrix}u\\ v\\ w\end{Bmatrix} \Rightarrow \mathbf{u}_1 = \mathbf{A}\,\mathbf{u} . \quad (6)$$

Due to the small thickness, it is common to assume that each layer of the plate is subjected to a Plane Stress State (PSS). Thus, all stress components parallel to the z-axis are zero. In this case, the deformation components of interest are given by.

ISSN: 2277-9655
Impact Factor: 5.164
CODEN: IJESS7

$$\boldsymbol{\varepsilon}=\begin{Bmatrix}\varepsilon_x\\ \varepsilon_y\\ \gamma_{xy}\end{Bmatrix}=\begin{Bmatrix}\dfrac{\partial u}{\partial x}\\ \dfrac{\partial v}{\partial y}\\ \dfrac{\partial u}{\partial y}+\dfrac{\partial v}{\partial x}\end{Bmatrix} \quad \text{e} \quad \boldsymbol{\varepsilon}_1=\begin{Bmatrix}\varepsilon_1\\ \varepsilon_2\\ \gamma_{12}\end{Bmatrix}=\begin{Bmatrix}\dfrac{\partial u_1}{\partial x_1}\\ \dfrac{\partial u_2}{\partial x_2}\\ \dfrac{\partial u_1}{\partial x_2}+\dfrac{\partial u_2}{\partial x_1}\end{Bmatrix}. \tag{7}$$

Using Equations (6) and (7) it can be shown that the membrane deformations can be transformed between the systems through the matrix relation:

$$\begin{Bmatrix}\varepsilon_1\\ \varepsilon_2\\ \gamma_{12}\end{Bmatrix}=\begin{bmatrix}\cos^2\theta & sen^2\theta & sen\theta\cos\theta\\ sen^2\theta & \cos^2\theta & -sen\theta\cos\theta\\ -2sen\theta\cos\theta & 2sen\theta\cos\theta & \cos^2\theta-sen^2\theta\end{bmatrix}\begin{Bmatrix}\varepsilon_{xx}\\ \varepsilon_{yy}\\ \gamma_{xy}\end{Bmatrix} \Rightarrow \boldsymbol{\varepsilon}_1=\mathbf{T}_m\,\boldsymbol{\varepsilon}. \tag{8}$$

The relation between tensions and membrane deformations can be obtained from Equation (2) by eliminating the null terms:

$$\begin{Bmatrix}\varepsilon_1\\ \varepsilon_2\\ \gamma_{12}\end{Bmatrix}=\begin{bmatrix}S_{11} & S_{12} & 0\\ S_{12} & S_{22} & 0\\ 0 & 0 & S_{66}\end{bmatrix}\begin{Bmatrix}\sigma_1\\ \sigma_2\\ \tau_{12}\end{Bmatrix} \tag{9}$$

where $S_{ij}$ coefficients are given by Equation (3). Finally, by inverting Equation (9), the stress-strain relationship can be written as

$$\begin{Bmatrix}\sigma_1\\ \sigma_2\\ \tau_{12}\end{Bmatrix}=\begin{bmatrix}Q_{11} & Q_{12} & 0\\ Q_{12} & Q_{22} & 0\\ 0 & 0 & Q_{66}\end{bmatrix}\begin{Bmatrix}\varepsilon_1\\ \varepsilon_2\\ \gamma_{12}\end{Bmatrix} \Rightarrow \boldsymbol{\sigma}_1=\mathbf{Q}\,\boldsymbol{\varepsilon}_1, \tag{10}$$

where the $Q_{ij}$ coefficients are calculated from the properties of the material, as follow:

$$Q_{11}=\frac{E_1}{1-\nu_{12}\nu_{21}},\quad Q_{12}=\frac{\nu_{12}E_2}{1-\nu_{12}\nu_{21}},\quad Q_{22}=\frac{E_2}{1-\nu_{12}\nu_{21}},\quad Q_{66}=G_{12}. \tag{11}$$

In relatively thick plates it is necessary to take into account the effect of transverse shear, which means that the $\tau_{23}$ and $\tau_{13}$ stresses should be considered. In this case, the shear deformations in the two systems are given by

$$\boldsymbol{\gamma}=\begin{Bmatrix}\gamma_{yz}\\ \gamma_{zx}\end{Bmatrix}=\begin{Bmatrix}\dfrac{\partial v}{\partial z}+\dfrac{\partial w}{\partial y}\\ \dfrac{\partial u}{\partial z}+\dfrac{\partial w}{\partial x}\end{Bmatrix} \quad \text{e} \quad \boldsymbol{\gamma}_1=\begin{Bmatrix}\gamma_{23}\\ \gamma_{31}\end{Bmatrix}=\begin{Bmatrix}\dfrac{\partial u_2}{\partial x_3}+\dfrac{\partial u_3}{\partial x_2}\\ \dfrac{\partial u_1}{\partial x_3}+\dfrac{\partial u_3}{\partial x_1}\end{Bmatrix}. \tag{12}$$

Using Equations (6) and (12), it is determined the transformation of the shear deformations between the two systems

ISSN: 2277-9655
Impact Factor: 5.164
CODEN: IJESS7

$$\begin{Bmatrix}\gamma_{23}\\ \gamma_{31}\end{Bmatrix}=\begin{bmatrix}\cos\theta & sen\,\theta\\ -sen\,\theta & \cos\theta\end{bmatrix}\begin{Bmatrix}\gamma_{yz}\\ \gamma_{zx}\end{Bmatrix}\ \Rightarrow\ \boldsymbol{\gamma}_1=\mathbf{T}_s\,\boldsymbol{\gamma}\,. \tag{13}$$

On the other hand, the stress-strain relationship due to transverse shear is given by:

$$\begin{Bmatrix}\tau_{23}\\ \tau_{31}\end{Bmatrix}=\begin{bmatrix}Q_{44} & 0\\ 0 & Q_{55}\end{bmatrix}\begin{Bmatrix}\gamma_{23}\\ \gamma_{31}\end{Bmatrix}\ \Rightarrow\ \boldsymbol{\tau}_1=\mathbf{Q}_s\,\boldsymbol{\gamma}_1, \tag{14}$$

Where

$$Q_{44}=G_{23}\ \text{ e }\ Q_{55}=G_{31}\ . \tag{15}$$

Using the Principle of Virtual Work it can be shown (Cook et al., 2002) that the transformation of local system stresses into the global system is done through:

$$\boldsymbol{\sigma}=\mathbf{T}_s^t\,\boldsymbol{\sigma}_1\ \text{ e }\ \boldsymbol{\tau}=\mathbf{T}_s^t\,\boldsymbol{\tau}_1. \tag{16}$$

Finally, substituting Equations (10), (8), (14) and (13), respectively in the first and second Equation (16), we get:

$$\begin{aligned}&\boldsymbol{\sigma}=\mathbf{T}_m{}^t\mathbf{Q}_m\mathbf{T}_m\,\boldsymbol{\varepsilon}\ \Rightarrow\ \boldsymbol{\sigma}=\overline{\mathbf{Q}}_m\,\boldsymbol{\varepsilon}\\ &\boldsymbol{\tau}=\mathbf{T}_s{}^t\mathbf{Q}_s\mathbf{T}_s\,\boldsymbol{\gamma}\ \Rightarrow\ \boldsymbol{\tau}=\overline{\mathbf{Q}}_s\,\boldsymbol{\gamma}\end{aligned} \tag{17}$$

Where

$$\overline{\mathbf{Q}}_m=\begin{bmatrix}\overline{Q}_{11} & \overline{Q}_{12} & \overline{Q}_{16}\\ \overline{Q}_{12} & \overline{Q}_{22} & \overline{Q}_{26}\\ \overline{Q}_{16} & \overline{Q}_{26} & \overline{Q}_{66}\end{bmatrix}\ \text{ e }\ \overline{\mathbf{Q}}_s=\begin{bmatrix}\overline{Q}_{44} & \overline{Q}_{45}\\ \overline{Q}_{45} & \overline{Q}_{55}\end{bmatrix} \tag{18}$$

The $\overline{Q}_{ij}$ coefficients are determined by performing the following matrix operations:

$$\begin{aligned}
\overline{Q}_{11}&=\cos^4\theta\,Q_{11}+2sen^2\theta\cos^2\theta\,(Q_{12}+2Q_{66})+sen^4\theta\,Q_{22}\\
\overline{Q}_{12}&=(Q_{11}+Q_{22}-4Q_{66})sen^2\theta\cos^2\theta+(sen^4\theta+\cos^4\theta)\,Q_{12}\\
\overline{Q}_{16}&=(Q_{11}-Q_{12}-2Q_{66})sen\ \theta\cos^3\theta+(Q_{12}-Q_{22}+2Q_{66})sen^3\theta\cos\ \theta\\
\overline{Q}_{22}&=sen^4\theta\,Q_{11}+2(Q_{12}+2Q_{66})sen^2\theta\cos^2\theta+\cos^4\theta\,Q_{22}\\
\overline{Q}_{26}&=(Q_{11}-Q_{12}-2Q_{66})sen^3\theta\cos\ \theta+(Q_{12}-Q_{22}+2Q_{66})sen\ \theta\cos^3\theta\\
\overline{Q}_{66}&=(Q_{11}+Q_{22}-2Q_{12}-2Q_{66})sen^2\theta\cos^2\theta+\ (sen^4\theta+\cos^4\theta)\,Q_{66}\\
\overline{Q}_{45}&=(Q_{55}-Q_{44})sen\theta\cos\theta\\
\overline{Q}_{44}&=\cos^2\theta\,Q_{44}+sen^2\theta\,Q_{55}\\
\overline{Q}_{55}&=sen^2\theta\,Q_{44}+\cos^2\theta\,Q_{55}
\end{aligned} \tag{19}$$

ISSN: 2277-9655
Impact Factor: 5.164
CODEN: IJESS7

The $\overline{\mathbf{Q}}$ matrix is called the transformed stiffness matrix, since it is in the global coordinate system.

$$\overline{\mathbf{Q}}=\begin{bmatrix}\overline{\mathbf{Q}}_m & 0\\ 0 & \overline{\mathbf{Q}}_s\end{bmatrix} \tag{20}$$

### *4. Analysis of laminated plates*

The deformations in the plane $x_1$, $y_1$ at a distance $z_1$ from the median plane of the plate are deformations due to bending. That can be represented by the partial derivatives, according to Szilard (2003) and thus to be determined the equations that govern the laminated plate and thick plate, according to Figure 4:

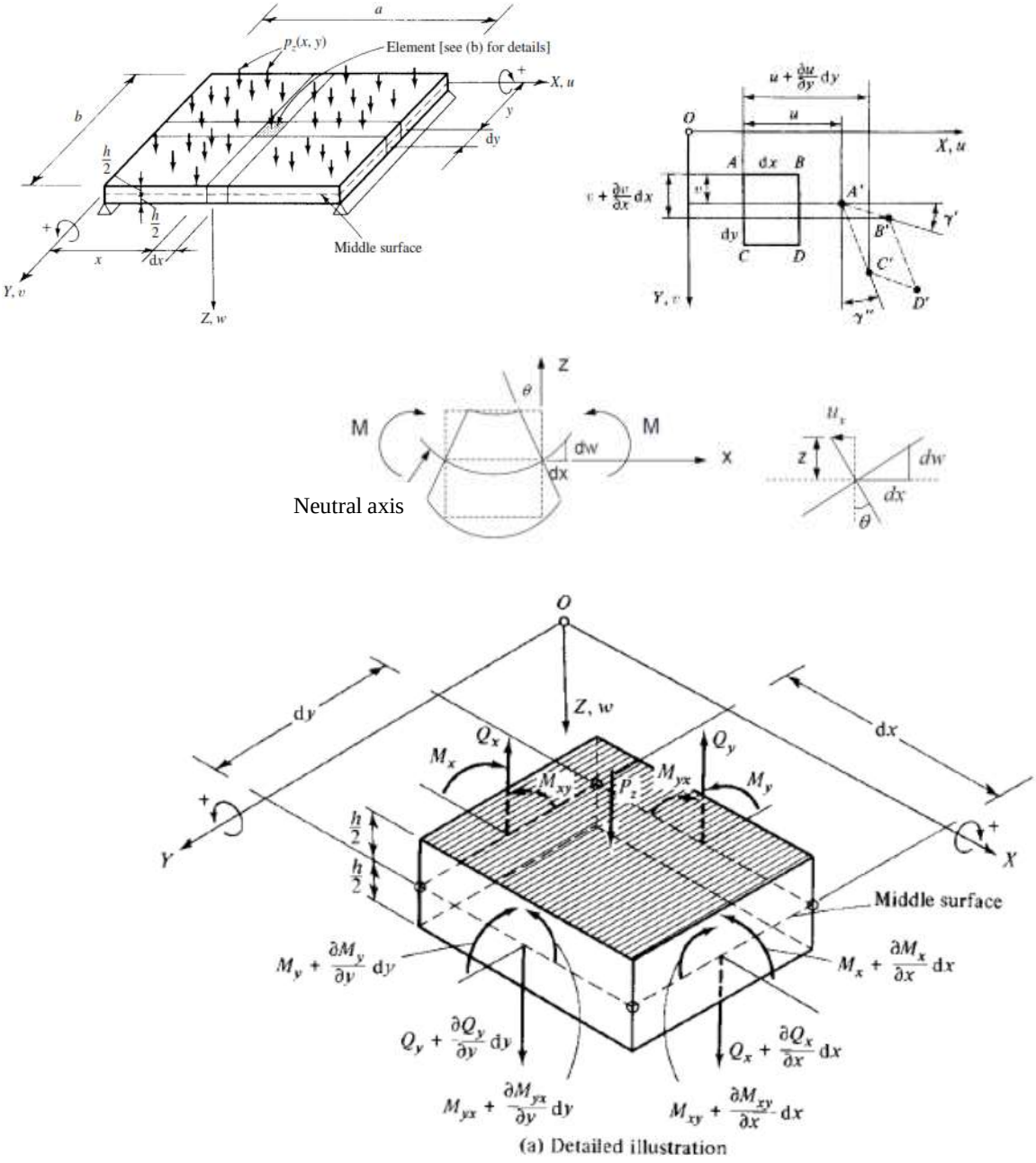

ISSN: 2277-9655
Impact Factor: 5.164
CODEN: IJESS7

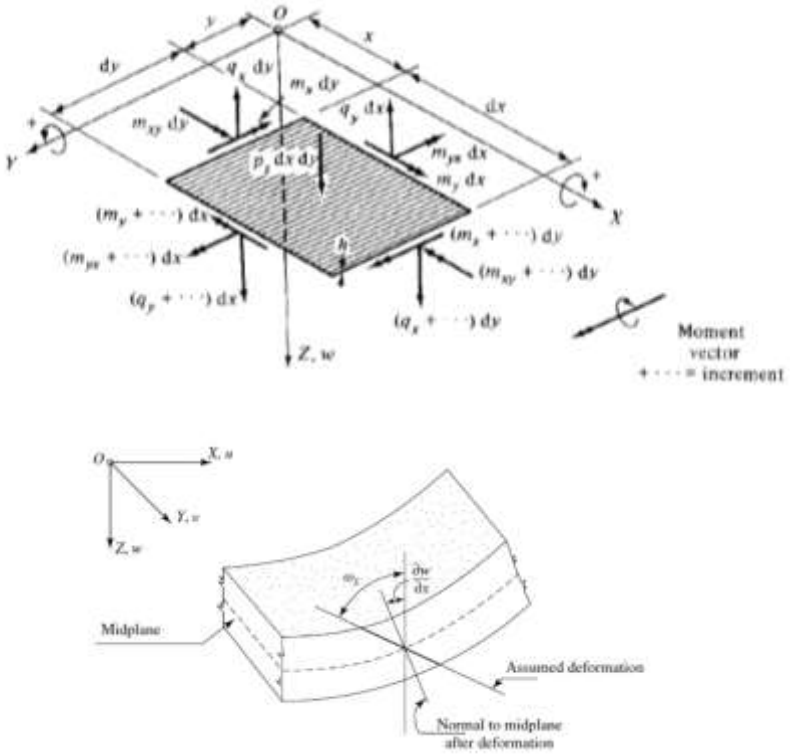


**Figure 4** - ***Deformed bisupported plate with distributed loading (Szilard, 2003)***

According to the classical plate theory (Kirchhoff's theory) a normal line to the median plane of the plate will remain normal to the median plate surface after deformation. This implies that the transverse shear effect is not considered, since the angular deformations ($\gamma_{xz}$ and $\gamma_{yz}$) are zero. This theory is appropriate only for homogeneous plates of small thickness.

In the case of thick plates and laminated plates, transverse shear cannot be neglected, requiring the use of another plate theory. In Mindlin's theory, the shear effect is considered roughly. The basic hypothesis of this theory is that a normal line to the median plane of the plate will not necessarily remain normal to the median plane of the plate after the deformation, as shown in Figure 5.

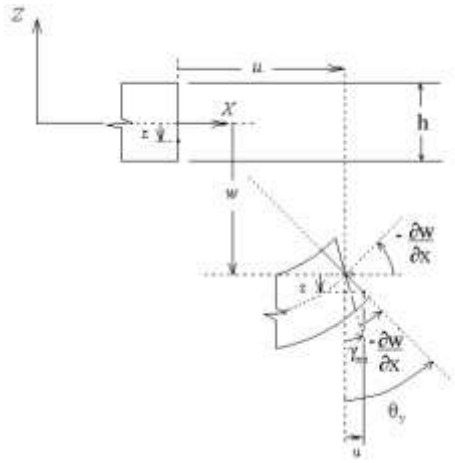


**Figure 5 – *Deformations in Mindlin's theory***

ISSN: 2277-9655
Impact Factor: 5.164
CODEN: IJESS7

According to this figure it is verified that the displacements at any point of the plate ($u_x, u_y$ and $u_z$) are given by:

$$u_x(x,y,z)=u(x,y)+z\theta_y \qquad u_y(x,y,z)=v(x,y)-z\theta_x \qquad u_z(x,y,z)=w(x,y) \tag{21}$$

where *u*, *v* and *w* are the transverse displacements of the median plane of the plate and $\theta_x$ e $\theta_y$ are the rotations of the normal line about the x and y axes respectively.

When the displacements are moderately large, there is an interaction between the effects of membrane and bending due to transverse displacements. Von Kármán's theory incorporates this effect using a simplified form of the Green-Lagrange deformations obtained by neglecting the nonlinear terms associated with the displacement components in the directions of the plate's plane, $u_x$ and $u_y$ (Crisfield, 1991). In this case, the deformation components at any point on the plate are:

$$\boldsymbol{\varepsilon} = \begin{Bmatrix} \varepsilon_x \\ \varepsilon_y \\ \gamma_{xy} \end{Bmatrix} = \begin{Bmatrix} \dfrac{\partial u_x}{\partial x} \\ \dfrac{\partial u_y}{\partial y} \\ \dfrac{\partial u_x}{\partial y} + \dfrac{\partial u_y}{\partial x} \end{Bmatrix} + \begin{Bmatrix} \dfrac{1}{2}\left(\dfrac{\partial u_z}{\partial x}\right)^2 \\ \dfrac{1}{2}\left(\dfrac{\partial u_z}{\partial y}\right)^2 \\ \left(\dfrac{\partial u_z}{\partial x}\right)\left(\dfrac{\partial u_z}{\partial y}\right) \end{Bmatrix}. \tag{22}$$

Replacing the displacement given by Eq. (21) in Eq. (22), we have that the deformations in any plane parallel to the median plane of the plate are given by:

$$\boldsymbol{\varepsilon} = \begin{Bmatrix} \varepsilon_x \\ \varepsilon_y \\ \gamma_{xy} \end{Bmatrix} = \begin{Bmatrix} \dfrac{\partial u}{\partial x} \\ \dfrac{\partial v}{\partial y} \\ \dfrac{\partial u}{\partial y} + \dfrac{\partial v}{\partial x} \end{Bmatrix} + \begin{Bmatrix} \dfrac{1}{2}\left(\dfrac{\partial w}{\partial x}\right)^2 \\ \dfrac{1}{2}\left(\dfrac{\partial w}{\partial y}\right)^2 \\ \left(\dfrac{\partial w}{\partial x}\right)\left(\dfrac{\partial w}{\partial y}\right) \end{Bmatrix} + z\begin{Bmatrix} \dfrac{\partial \theta_y}{\partial x} \\ -\dfrac{\partial \theta_x}{\partial y} \\ \dfrac{\partial \theta_y}{\partial y} - \dfrac{\partial \theta_x}{\partial x} \end{Bmatrix} \tag{23}$$

The first two portions correspond to the membrane deformations and the third portion due to the bending components. These deformations can be written matrically as:

$$\boldsymbol{\varepsilon} = \boldsymbol{\varepsilon}^{\mathbf{m}} + z\boldsymbol{\kappa} \tag{24}$$

where $\boldsymbol{\varepsilon}^{\mathbf{m}}$ is the deformation of the median plane's membrane and is associated with the curvature of the plate.

Membrane deformations are composed of two portions, the first due to linear behavior and the second due to the nonlinear effect of the transverse displacements of the plate, as shown in Eq. (25). Using the matrix notation, we have:

$$\boldsymbol{\varepsilon}^m = \boldsymbol{\varepsilon}_0^m + \boldsymbol{\varepsilon}_L^m \tag{25}$$

On the other hand, the deformations due to the transversal shear are given by:

ISSN: 2277-9655
Impact Factor: 5.164
CODEN: IJESS7

$$\boldsymbol{\gamma}=\begin{Bmatrix}\gamma_{xz}\\ \gamma_{yz}\end{Bmatrix}=\begin{Bmatrix}\left(\dfrac{\partial w}{\partial x}+\theta_y\right)\\ \left(\dfrac{\partial w}{\partial y}-\theta_x\right)\end{Bmatrix} \tag{26}$$

For a generic layer *k* with unidirectional fibers, as shown in Figure 3, the tensions are given by Eq. (17) and the components of $\overline{\mathbf{Q}}_m^k$ and $\overline{\mathbf{Q}}_s^k$ are given by Eq. (19).

The resulting forces and moments (generalized tensions) are obtained by integrating the stresses along the thickness of the plate:

$$\mathbf{N}=\begin{Bmatrix}N_x\\ N_y\\ N_{xy}\end{Bmatrix}=\int_{-h/2}^{h/2}\begin{Bmatrix}\sigma_x\\ \sigma_y\\ \tau_{xy}\end{Bmatrix}dz,\quad \mathbf{M}=\begin{Bmatrix}M_x\\ M_y\\ M_{xy}\end{Bmatrix}=\int_{-h/2}^{h/2}\begin{Bmatrix}\sigma_x\\ \sigma_y\\ \tau_{xy}\end{Bmatrix}z\,dz,\quad \mathbf{Q}=\begin{Bmatrix}Q_{xz}\\ Q_{yz}\end{Bmatrix}=\int_{-h/2}^{h/2}\begin{Bmatrix}\tau_{xz}\\ \tau_{yz}\end{Bmatrix}dz \tag{27}$$

It is important to note that, according to Eqs. (22) and (24), the deformations are continuous along the thickness of the layer, regardless the material variation, which does not occur with the stress components, as shown in Eq. (17). In general, this is due to the change in the properties of each layer. Using Eqs. (17) and (24) in (27), it can be written in terms of internal stresses and generalized deformations:

$$\boldsymbol{\sigma}=\mathbf{C}\,\boldsymbol{\varepsilon}\quad\Rightarrow\quad\begin{Bmatrix}\mathbf{N}\\ \mathbf{M}\\ \mathbf{Q}\end{Bmatrix}=\begin{bmatrix}\mathbf{A}&\mathbf{B}&\mathbf{0}\\ \mathbf{B}&\mathbf{D}&\mathbf{0}\\ \mathbf{0}&\mathbf{0}&\mathbf{G}\end{bmatrix}\begin{Bmatrix}\boldsymbol{\varepsilon}^m\\ \boldsymbol{\kappa}\\ \boldsymbol{\gamma}\end{Bmatrix} \tag{28}$$

where the sub-matrix components are given by

$$A_{ij}=\sum_{l=1}^{n}\overline{Q}_{ij}^k\left(z_{l+1}-z_l\right)\quad B_{ij}=\sum_{l=1}^{n}\frac{\overline{Q}_{ij}^k\left(z_{l+1}^2-z_l^2\right)}{2}\quad D_{ij}=\sum_{l=1}^{n}\frac{\overline{Q}_{ij}^k\left(z_{l+1}^3-z_l^3\right)}{3}\quad i,j=1,2e6$$
$$G_{ij}=\sum_{l=1}^{n}k_{ij}\overline{Q}_{ij}^k\left(z_{l+1}-z_l\right)\quad i,j=4e5 \tag{29}$$

and $k_{ij}$ is the correction factor of shear stresses (Reddy, 1996). It is found that if the laminated plate is symmetrical, the matrix B is zero.

### *5. Non-linear geometric analysis*

Several problems of practical interest can be easily solved considering linear models, which present satisfactory approximate results when displacements and deformations are small. However, when the displacements and deformations begin to increase, the effects of geometric non-linearity must be considered in the structure analysis. This is also the case for structures that undergo buckling by bifurcation even when the displacements are small, such as perfect columns and plates and loaded in their own plane.

In non-linear geometrical problems, the analysis can be performed starting from the initial configuration of the structure and determining the displacements, stresses and stresses as the load is increased. This strategy is known as Load Control (Crisfield, 1991), where interative load increments are applied in order to determine the equilibrium path of the structure. Due to the nonlinearity of the response it is necessary to use an iterative procedure to determine the displacements corresponding to the applied load. One of the most used methods for this purpose is the Newton-Raphson's method (Crisfield, 1991, Bathe, 1996, Cook et al., 2002), since this one presents quadratic convergence.

ISSN: 2277-9655
Impact Factor: 5.164
CODEN: IJESS7

The equilibrium equations of the structural system can be written as (Crisfield, 1991):

$$\mathbf{r(u)} = \mathbf{g(u)} - \lambda \mathbf{f} = \mathbf{0} \tag{30}$$

where **u** is the nodal displacement vector, **r** is the vector of unbalanced forces (residual), **g** is the vector of internal forces, **f** is the vector of external forces, and λ is the load factor. Note that in this equation the total load is given by the product between the load factor and the reference loads. Increasing the load factor, it is possible to control the variation of the total external force.

Using the Principle of Virtual Works (PVW), we have:

$$\delta W_{\text{int}} = \delta W_{ext} \tag{31}$$

The external virtual work leads to the vector of equivalent nodal forces in a process that is essentially the same as the one used in linear problems. On the other hand, internal work leads to the determination of the vector of internal forces

$$\delta W_{\text{int}} = \int_V \delta\boldsymbol{\varepsilon}^t \, \boldsymbol{\sigma} \, dV = \delta \mathbf{u}^t \mathbf{g} \;\Rightarrow\; \mathbf{g} = \int_V \overline{\mathbf{B}}^t \, \boldsymbol{\sigma} \, dV \tag{32}$$

where the $\overline{\mathbf{B}}$ matrix is defined through the relation

$$\delta\boldsymbol{\varepsilon} = \overline{\mathbf{B}} \, \delta\mathbf{u} \tag{33}$$

Using the Newton-Raphson method, the vector of internal forces **g(u)** is linearized with respect to the displacements du. Therefore:

$$d\mathbf{g} = \int_V \overline{\mathbf{B}}^t \, d\boldsymbol{\sigma} \, dV + \int_V d\overline{\mathbf{B}}^t \, \boldsymbol{\sigma} \, dV = \mathbf{K}_t \, d\mathbf{u} \tag{34}$$

where $\mathbf{K}_t$ is the tangent stiffness matrix. Using Eqs. (1) and (33), it is verified that the stress increase is given by:

$$d\boldsymbol{\sigma} = \mathbf{C} \, d\boldsymbol{\varepsilon} = \mathbf{C}\overline{\mathbf{B}} \, d\mathbf{u} \tag{35}$$

and from Equation (50):

$$d\overline{\mathbf{B}} = d\overline{\mathbf{B}}_L \tag{36}$$

Substituting Eqs. (35) and (36) into Eq. (34), we have:

$$d\mathbf{g} = \int_V \overline{\mathbf{B}}^t \mathbf{C} \overline{\mathbf{B}} \, dV \, d\mathbf{u} + \int_V d\overline{\mathbf{B}}_L^t \boldsymbol{\sigma} \, dV = (\mathbf{K}_e + \mathbf{K}_\sigma) d\mathbf{u} \;\Rightarrow\; \mathbf{K}_t = \mathbf{K}_e + \mathbf{K}_\sigma \tag{37}$$

where $\mathbf{K}_e$ is known as the elastic stiffness matrix and $\mathbf{K}_\sigma$ is known as the geometric stiffness matrix or the initial stresses (Crisfield, 1991; Zienkiewicz and Taylor, 2000). From Eqs. (50) and (34) it can be seen that this matrix can be written as

$$\mathbf{K}_e = \int_V \overline{\mathbf{B}}^t \mathbf{C} \overline{\mathbf{B}} \, dV = \mathbf{K}_0 + \mathbf{K}_L \tag{38}$$

Thus, elastic stiffness matrix is obtained by summing the initial stiffness matrix ( $\mathbf{K}_0$ ) and the stiffness matrix due to the previous displacements ( $\mathbf{K}_L$ ).

ISSN: 2277-9655
Impact Factor: 5.164
CODEN: IJESS7

### *6. Isoparametric elements*

It is important to note that the elastic matrix shown in Eq. (38) is independent of the finite element used. However, the same does not occur with the $\overline{\mathbf{B}}$ and Kσ matrices. Thus, the complete definition of the matrices to be used in the analysis of the stability of laminated plates requires the specification of the finite element used.
In this work, isoparametric finite elements were used (Cook et al., 2002). It is important to note that, due to the use of Mindlin's theory, only interpolation functions need to be continuous between the elements. Therefore, continuity functions $C^0$ can be used (Cook et al, 2002), which greatly simplifies the formulation of FEM.

In the isoparametric formulation, the displacements in the finite element are interpolated independently from the nodal displacements. According to Equations (22) and (24), the elements have 5 degrees of freedom per node, which are the transverse displacements *u*, *v* and *w* and the rotations $\theta_x$ and $\theta_y$. Like this,

$$u=\sum_{i=1}^{n}N_i u_i \quad v=\sum_{i=1}^{n}N_i v_i \quad w=\sum_{i=1}^{n}N_i w_i \quad \theta_x=\sum_{i=1}^{n}N_i \theta_{xi} \quad \theta_y=\sum_{i=1}^{n}N_i \theta_{y_i} \tag{39}$$

where *n* is the number of nodes and $N_i$ are the shape (interpolation) functions of the element.

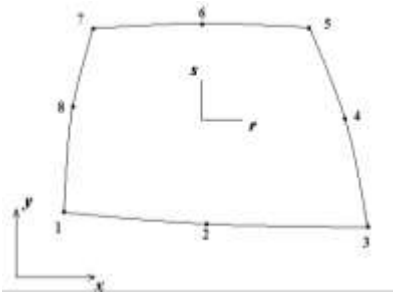

**Figure 6 – Isoparametric finite element**

In order to allow for curved elements, as shown in Figure 5, the isoparametric formulation interpolates the geometry of the element by means of the same interpolation functions of the displacement. Like this:

$$x=\sum_{i=1}^{n}N_i x_i \quad \text{e} \quad y=\sum_{i=1}^{n}N_i y_i \tag{40}$$

From Eq. (23) it is verified that the deformations are the sum of a linear portion and a quadratic portion. Using a matrix notation, the total deformations can be written as

$$\boldsymbol{\varepsilon}=\mathbf{B}_0\mathbf{u}+\frac{1}{2}\mathbf{B}_L(\mathbf{u})\mathbf{u} \tag{41}$$

where $\mathbf{B}_0$ is a constant matrix that relates the displacements to the infinitesimal deformations and $\mathbf{B}_L$ relates the nonlinear portion of the deformations to the nodal displacements (**u**). The $\mathbf{B}_L$ matrix depends linearly on the nodal displacements.

Using Equations (24), (33) and (39), it can be shown that the matrix is given by:

$$\mathbf{B}_0=\begin{bmatrix}\mathbf{B}_0^m\\ \mathbf{B}_0^b\\ \mathbf{B}_0^s\end{bmatrix} \tag{42}$$

ISSN: 2277-9655
Impact Factor: 5.164
CODEN: IJESS7

where $\mathbf{B}_0^m$ is the portion of membrane, $\mathbf{B}_0^b$ is the portion of bending and $\mathbf{B}_0^s$ is the portion of shear. In the isoparametric formulation these matrices are composed of a set of submatrices corresponding to each node of the element. Thus, considering only the submatrices referring to *i* node, we have:

$$\boldsymbol{\varepsilon}_0^m = \sum_{i=1}^{n} \begin{bmatrix} \frac{\partial N_i}{\partial x} & 0 & 0 & 0 & 0 \\ 0 & \frac{\partial N_i}{\partial y} & 0 & 0 & 0 \\ \frac{\partial N_i}{\partial y} & \frac{\partial N_i}{\partial x} & 0 & 0 & 0 \end{bmatrix} \begin{Bmatrix} u_i \\ v_i \\ w_i \\ \theta_{x_i} \\ \theta_{y_i} \end{Bmatrix} \Rightarrow \boldsymbol{\varepsilon}_0^m = \mathbf{B}_0^m \mathbf{u} \tag{43}$$

$$\boldsymbol{\kappa} = \sum_{i=1}^{n} \begin{bmatrix} 0 & 0 & 0 & 0 & \frac{\partial N_i}{\partial x} \\ 0 & 0 & 0 & -\frac{\partial N_i}{\partial y} & 0 \\ 0 & 0 & 0 & -\frac{\partial N_i}{\partial x} & \frac{\partial N_i}{\partial y} \end{bmatrix} \begin{Bmatrix} u_i \\ v_i \\ w_i \\ \theta_{x_i} \\ \theta_{y_i} \end{Bmatrix} \Rightarrow \boldsymbol{\kappa} = \mathbf{B}_0^b \mathbf{u} \tag{44}$$

$$\boldsymbol{\gamma} = \sum_{i=1}^{n} \begin{bmatrix} 0 & 0 & \frac{\partial N_i}{\partial x} & 0 & N_i \\ 0 & 0 & \frac{\partial N_i}{\partial y} & -N_i & 0 \end{bmatrix} \begin{Bmatrix} u_i \\ v_i \\ w_i \\ \theta_{x_i} \\ \theta_{y_i} \end{Bmatrix} \Rightarrow \boldsymbol{\gamma} = \mathbf{B}_0^s \mathbf{u} \tag{45}$$

As for the nonlinear portion of the deformation, using Equations (26), (33) and (39), it is verified that the $\mathbf{B}_L$ matrix is given by:

$$\mathbf{B}_L = \begin{bmatrix} \mathbf{B}_L^m \\ 0 \\ 0 \end{bmatrix}, \tag{46}$$

Since, according to von Kármán's theory, only the membrane deformations depend quadratically on the displacements. From Eq. (23) these deformations can be written as:

$$\boldsymbol{\varepsilon}_L^m = \frac{1}{2} \begin{bmatrix} \frac{\partial w}{\partial x} & 0 \\ 0 & \frac{\partial w}{\partial y} \\ \frac{\partial w}{\partial x} & \frac{\partial w}{\partial y} \end{bmatrix} \begin{Bmatrix} \frac{\partial w}{\partial x} \\ \frac{\partial w}{\partial y} \end{Bmatrix} = \frac{1}{2} \mathbf{A}\boldsymbol{\beta} \ , \tag{47}$$

Where the vector **β**, which contains the derivatives of the transverse displacements, can be written as:

ISSN: 2277-9655
Impact Factor: 5.164
CODEN: IJESS7

$$\boldsymbol{\beta}=\begin{Bmatrix}\beta_x\\ \beta_y\end{Bmatrix}=\begin{Bmatrix}\frac{\partial w}{\partial x}\\ \frac{\partial w}{\partial y}\end{Bmatrix}=\sum_{i=1}^{n}\begin{bmatrix}0 & 0 & \frac{\partial N_i}{\partial x} & 0 & 0\\ 0 & 0 & \frac{\partial N_i}{\partial y} & 0 & 0\end{bmatrix}\begin{Bmatrix}u_i\\ v_i\\ w_i\\ \theta_{x_i}\\ \theta_{y_i}\end{Bmatrix}=\sum_{i=1}^{n}\mathbf{G}_i\mathbf{u}_i \Rightarrow \boldsymbol{\beta}=\mathbf{G}\mathbf{u} \tag{48}$$

Then, according to Equations (47) and (48), we can write:

$$\boldsymbol{\varepsilon}_L^m=\frac{1}{2}\sum_{i=1}^{n}\begin{bmatrix}0 & 0 & \frac{\partial N_i}{\partial x}\beta_x & 0 & 0\\ 0 & 0 & \frac{\partial N_i}{\partial y}\beta_y & 0 & 0\\ 0 & 0 & \frac{\partial N_i}{\partial x}\beta_y+\frac{\partial N_i}{\partial y}\beta_x & 0 & 0\end{bmatrix}\begin{Bmatrix}u_i\\ v_i\\ w_i\\ \theta_{x_i}\\ \theta_{y_i}\end{Bmatrix}=\sum_{i=1}^{n}\mathbf{B}_{L\,i}^m\mathbf{u}_i \Rightarrow \boldsymbol{\varepsilon}_L^m=\frac{1}{2}\mathbf{B}_L^m\mathbf{u} \tag{49}$$

The $\overline{\mathbf{B}}$ matrix relates the deformation increments inside the element with the increment of nodal displacements. From Eqs. (33), (42), (41) and (46) we easily get

$$\overline{\mathbf{B}}=\mathbf{B}_0+\mathbf{B}_L(\mathbf{u}) \tag{50}$$

With this matrix, all the terms needed to determine the stiffness matrix have already been obtained.

In order to obtain the tangent stiffness matrix, it is necessary to determine the geometric stiffness matrix. According to Eqs. (37) and (46):

$$\mathbf{K}_\sigma\, d\mathbf{u}=\int_V d\overline{\mathbf{B}}_L^t\boldsymbol{\sigma}\,dV=\int_A d\mathbf{B}_L^{m\,T}\boldsymbol{\sigma}^m\,dA \tag{51}$$

From Eq. (46) we have

$$d\mathbf{B}_L^m=d\mathbf{A}\,\mathbf{G} \tag{52}$$

Then, the substitution of Equation (52) in Equation (51) leads to

$$\mathbf{K}_\sigma\, d\mathbf{u}=\int_A \mathbf{G}^T d\mathbf{A}^T\boldsymbol{\sigma}^m\,dA \tag{53}$$

It is known that:

$$d\mathbf{A}^T\boldsymbol{\sigma}^m=\begin{bmatrix}\frac{\partial dw}{\partial x} & 0 & \frac{\partial dw}{\partial y}\\ 0 & \frac{\partial dw}{\partial y} & \frac{\partial dw}{\partial x}\end{bmatrix}\begin{Bmatrix}N_x\\ N_x\\ N_{xy}\end{Bmatrix}=\begin{bmatrix}N_x & N_{xy}\\ N_{xy} & N_y\end{bmatrix}\begin{Bmatrix}\frac{\partial dw}{\partial x}\\ \frac{\partial dw}{\partial y}\end{Bmatrix}=\begin{bmatrix}N_x & N_{xy}\\ N_{xy} & N_y\end{bmatrix}d\boldsymbol{\beta} \tag{54}$$

where $d\boldsymbol{\beta}$ is found by deriving Equation (48) in relation to the displacements.

$$d\boldsymbol{\beta}=\mathbf{G}\,d\mathbf{u} \tag{55}$$

Substituting Equation (55) into Equation (54), we have:

ISSN: 2277-9655
Impact Factor: 5.164
CODEN: IJESS7

$$dA^T \boldsymbol{\sigma}^m = \begin{bmatrix} N_x & N_{xy} \\ N_{xy} & N_y \end{bmatrix} \mathbf{G}\, d\mathbf{u} = \mathbf{S}\, \mathbf{G}\, d\mathbf{u} \;\Rightarrow\; \mathbf{S} = \begin{bmatrix} N_x & N_{xy} \\ N_{xy} & N_y \end{bmatrix} \tag{56}$$

Finally, replacing Equation (56) in Equation (53), we obtain the expression of the geometric stiffness matrix:

$$\mathbf{K}_\sigma = \int_A \mathbf{G}^T \mathbf{S}\, \mathbf{G}\, dA \tag{57}$$

It is verified that this matrix is symmetric since the matrix **S** is symmetrical by construction.

### *7. Calculation of critical loads*

If the internal forces vector and the tangent stiffness matrix are determined, the nonlinear path of laminated plates can be obtained by using appropriate methods such as the Load Control Method or the Arc Length Method (Crisfield, 1991). However, in this work the objective is only to obtain the linearized critical load of the structure through the solution of a generalized eigenvalue problem (Bathe, 1996; Cook et al., 2002).

In this case, a linear analysis of the structure submitted to the **f** reference load is carried out initially to determine the tensions and the $\overline{\mathbf{K}}_\sigma$ corresponding geometric stiffness matrix. Assuming that the pre-critical displacements are negligible, the stresses distribution remains constant if the load is multiplied by a load factor λ, with the corresponding stresses being obtained by multiplying the reference stresses by this factor. The same occurs with the geometric rigidity:

$$\mathbf{K}_\sigma = \lambda \overline{\mathbf{K}}_\sigma \tag{58}$$

It is also noticed that, neglecting the pre-critical displacements, the elastic stiffness matrix reduces to the initial stiffness matrix $\mathbf{K}_0$.

It is necessary that the tangent stiffness matrix be singular for buckling to occur:

$$|\mathbf{K}_t| = 0 \;\Rightarrow\; |\mathbf{K}_0 + \lambda_{cr}\, \overline{\mathbf{K}}_\sigma| = 0\,. \tag{59}$$

Alternatively, the critical points are characterized by the condition that at least one eigenvalue of the tangent stiffness matrix must be null. Therefore, the critical load can be calculated by solving the generalized eigenvalue problem:

$$(\mathbf{K}_0 + \lambda_{cr}\, \overline{\mathbf{K}}_\sigma)\mathbf{v} = 0, \quad |\mathbf{v}| \neq 0 \tag{60}$$

In this equation, the $\lambda_{cr}$ eigenvalue represents the critical load factor and the **v** eigenvector represents the associated buckling mode.

## III. NUMERICAL EXAMPLES

The formulation described in the previous items was implemented in the Matlab software (Martha and Parente, 2002). In this section are given examples of calculation of critical loads of laminated plates, these plates can represent ceramic tile applied on flat surface. The results of the present formulation will be compared with the analytical results obtained from Navier's solution for thin plates (Reddy, 1996) and the ABAQUS finite element commercial software.

Laminated plates subjected to only loads in their own plane shall be considered. According to Figure 6, the forces considered are:

ISSN: 2277-9655
Impact Factor: 5.164
CODEN: IJESS7

$$\hat{N}_{xx} = -N_o, \quad \hat{N}_{yy} = -kN_o, \quad k = \frac{\hat{N}_{yy}}{\hat{N}_{xx}} \tag{61}$$

Both uniaxial and biaxial compression plates will be considered, as shown in Figure 6 (a). For plates subjected to uniaxial loading, Equation (61) is given by:

$$\hat{N}_{xx} = -N_o, \quad \hat{N}_{yy} = 0, \quad k = 0 \tag{62}$$

and for biaxial loading, Figure 6 (b), Equation (61) is given by:

$$\hat{N}_{xx} = -N_0, \quad \hat{N}_{yy} = kN_0, \quad k = 1 \tag{63}$$

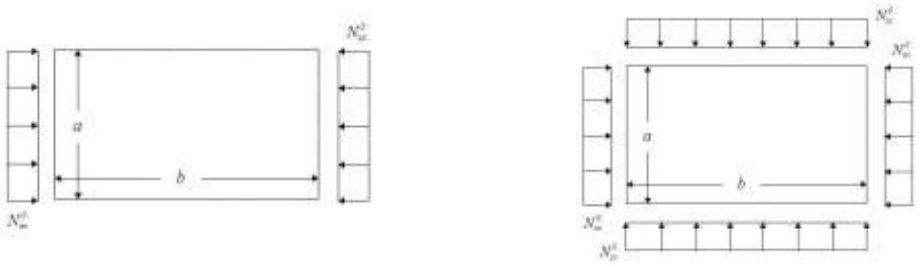

a) Uniaxial load b) Biaxial load

**Figure 7** – ***Load cases***

In all examples, a mesh composed of 10x10 quadratic quadrilateral elements (Q8) was used, as shown in Figure 7. In order to reduce shear lockage, the reduced integration technique with 2x2 Gauss points was used (Cook et al., 2002). Plates formed of two types of materials were analyzed and the same thickness was used for all examples.

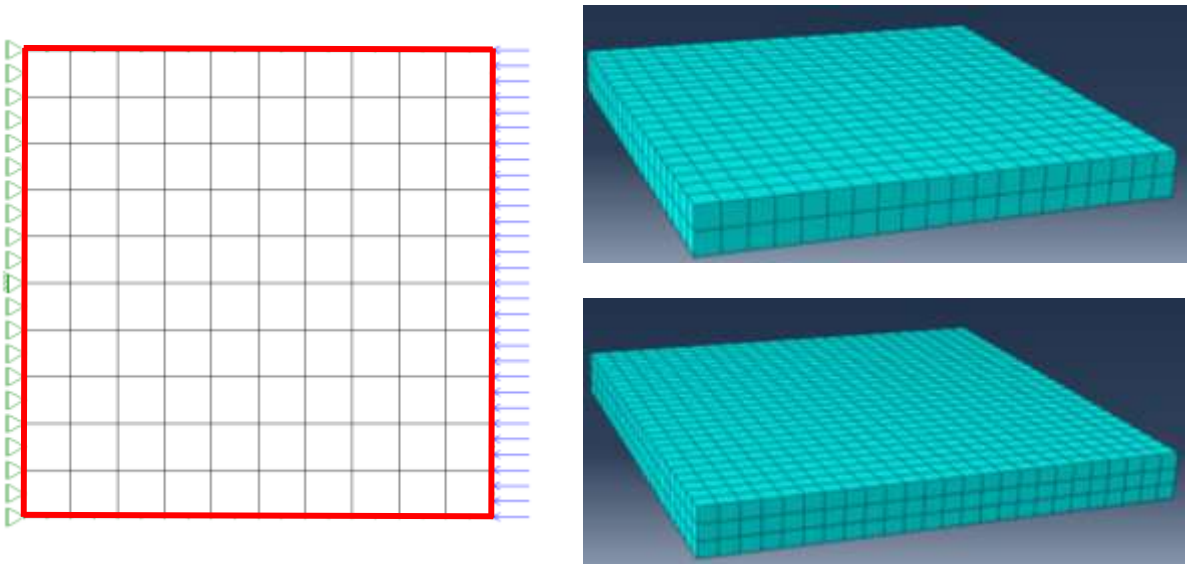

ISSN: 2277-9655
Impact Factor: 5.164
CODEN: IJESS7

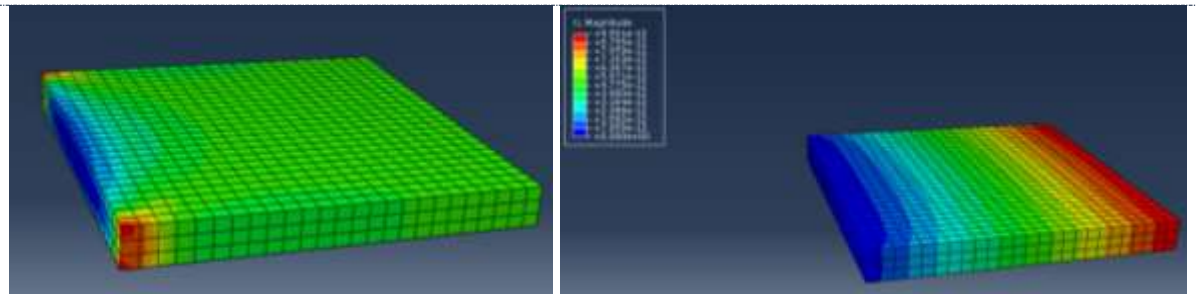

**Figure 8 –** ***Finite element mesh***

### *1. Symmetrical Laminated Plate*

The plate of Figure 7 is square (a / b = 1), *L* side equal to 2.0 m, *h* thickness equal to 0.02 m, formed by layers of the same thickness and material. Recalling that, for the uniaxial loading factor k = 0 and for biaxial loading k = 1, two materials with the following relations were considered:

$$E_1 = 25E_2 \quad G_{12} = G_{13} = 0.5E_2 \quad G_{23} = 0.2E_2 \quad \upsilon_{12} = 0.25 \tag{64}$$

$$E_1 = 40E_2 \quad G_{12} = G_{13} = 0.5E_2 \quad G_{23} = 0.2E_2 \quad \upsilon_{12} = 0.25 \tag{65}$$

For symmetric plates there is no membrane coupling, since matrix **B** is zero due to symmetry. The obtained results are dimensionless in as $\overline{N} = N_{cr}\left(b^2/\pi^2 D_{22}\right)$, (Reddy, 1996). The analytical solution was programmed in Matlab for different laminar plates as shown in Figure 9.

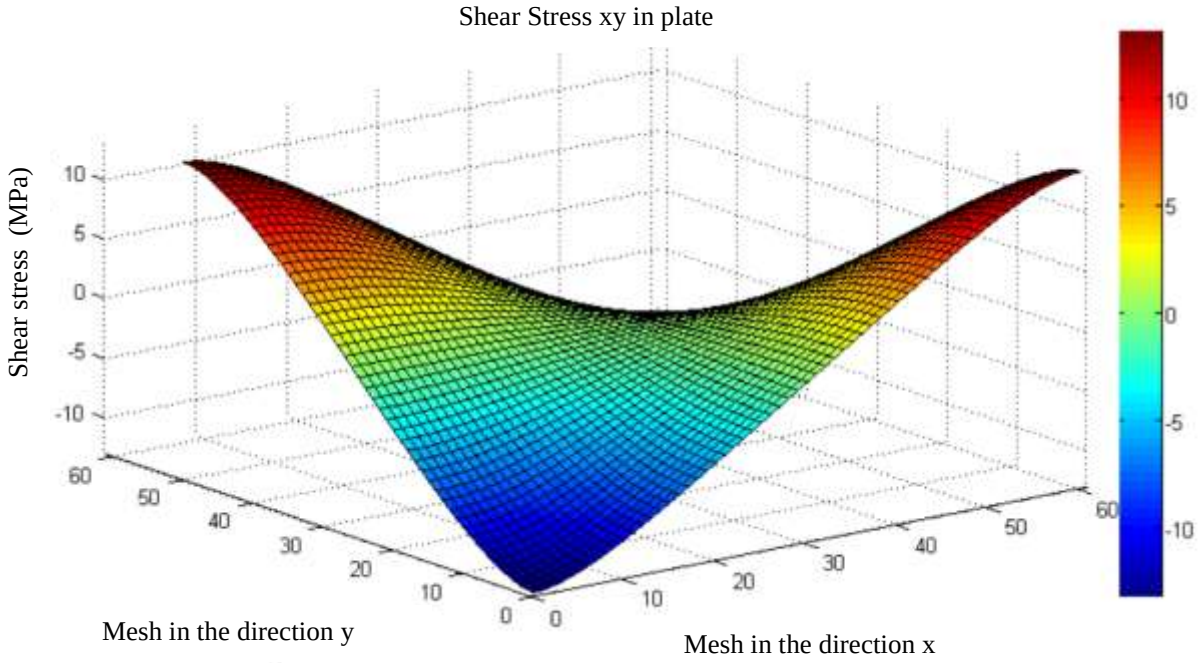

ISSN: 2277-9655
Impact Factor: 5.164
CODEN: IJESS7

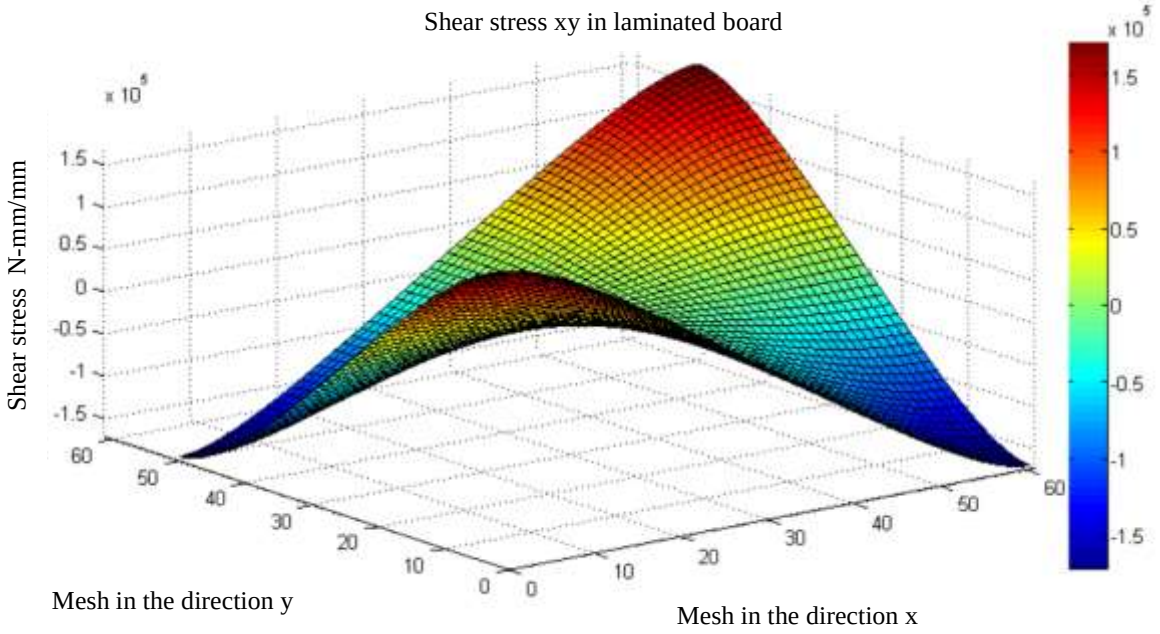


**Figure 9-** ***Analytical solution using Matlab***

The result obtained by the element implemented in Matlab converges perfectly for the analytical solution, both for Material 1 and Material 2. It is verified that, in this case, an excellent agreement with the theory is obtained, as expected given it is a thin plate. It is also observed that the results are very close to those obtained by ABAQUS, validating the formulation and implementation of the element.

### *2. Cross-ply anti-symmetrical laminated plate*

For a cross-ply anti-symmetric lamination plate, as shown in Figure 9, there is membrane-bending coupling because the anti-symmetry causes some elements of matrix **B** to be non-zero.

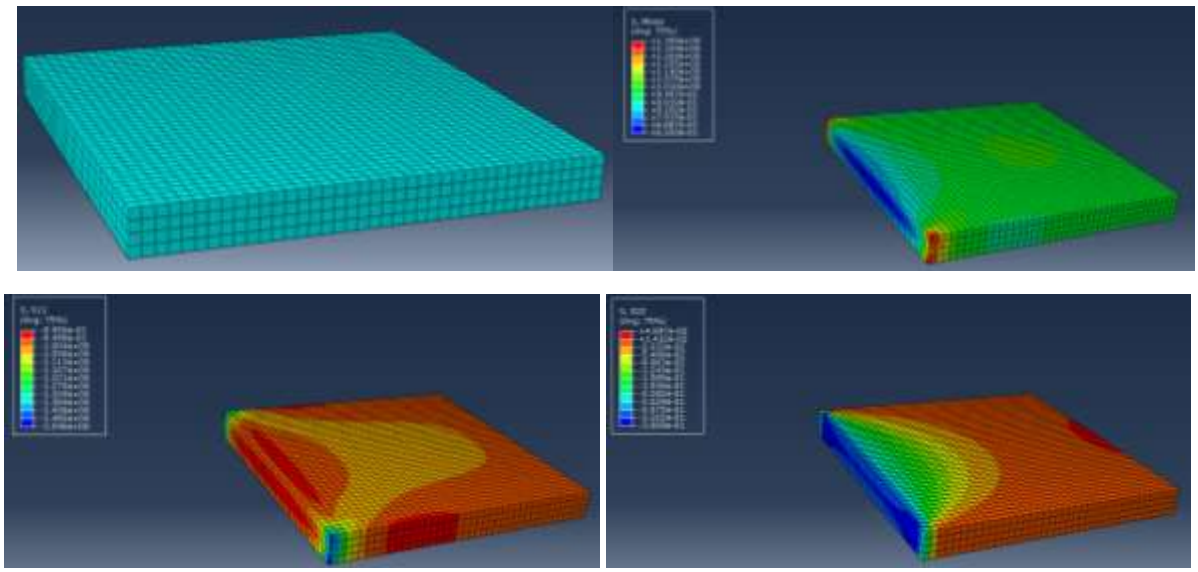

ISSN: 2277-9655
Impact Factor: 5.164
CODEN: IJESS7

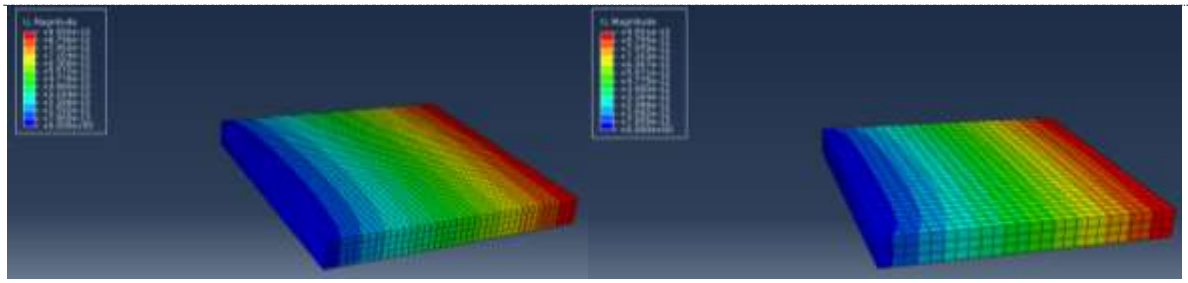

**Figure 9** - ***Modeling of the laminated board with different modulus of elasticity***

Table 1 shows the results of the analytical solution, in ABAQUS's solutions for the two types of material and loads for a *cross-ply* $(0/90)_2$ laminated plate. The obtained results are dimensionless as $\overline{N} = N_{cr}\left(b^2/\pi^2 D_{22}\right)$, (Reddy, 1996).

**Table 1 – Analytical solution, Matlab e ABAQUS's solution for the plate $(0/90)_2$.**

| E1/E2 | Analytical | Galerkin | Abaqus | Error Galerkin | Error Abaqus |
|---|---|---|---|---|---|
| Uniaxial Compression (k = 0) | | | | | |
| 25 | 1.866 | 1.870 | 1.857 | 0.20% | -0.50% |
| 40 | 1.778 | 1.777 | 1.764 | -0.03% | -0.81% |
| Biaxial Compression (k = 1) | | | | | |
| 25 | 0.933 | 0.930 | 0.928 | -0.32% | -0.52% |
| 40 | 0.889 | 0.885 | 0.882 | -0.50% | -0.81% |

It is verified that the result obtained by the element implemented in Abaqus for this case also converges perfectly for the analytical solution, for both materials. It is also noted that the results show good agreement with those obtained by ABAQUS, validating the formulation and implementation of the element.

## IV. CONCLUSIONS

This paper discussed a formulation for stability analysis of laminated plates through the Finite Element Method. The formulation presented allows the use of triangular and quadrilateral elements with different interpolation orders. In the numerical examples, the quadratic finite element with quadratic interpolation C3D8R was used to study its behavior. The reduced integration technique was used to alleviate the problem of shear locking.

The behavior of these elements was evaluated by comparing the results obtained by FEM with analytical solutions based on classical theory of laminated plates. The results show that the elements provided excellent accuracy results for both cross-ply and angle-ply laminated plates and uni and biaxial loading.

The example with symmetrical laminated plates presented excellent results, showing good agreement with the classical plate theory, as expected. It is interesting to note that by maintaining the thickness of the board, material and number of layers, only changing the layer structure the critical load of the symmetrical laminate is greater than the critical load of the *cross-ply* anti-symmetric laminate.

Another interesting aspect is the low reduction of the critical load when the E1 / E2 ratio is increased for both laminated structures. This aspect is important in defining the design of the layer, which will be determined from the characteristics and requirements of the project.

The examples with *angle-ply* anti-symmetrical laminated plates showed good results for both material and loading. Note that when increasing the number of layers, from two to eight, while maintaining the thickness of the plate, there is a considerable increase in the value of the critical load. This is a very important observation for the design of laminated plates subjected to compressive loads.

ISSN: 2277-9655
Impact Factor: 5.164
CODEN: IJESS7

It is observed that the critical load also increases for the *angle-ply* symmetrical and anti-symmetrical laminated structure, when the E1 / E2 ratio increases, in contrast to the *cross-ply* anti-symmetric laminated structure that decreases. Another important observation is about the type of loading, where it is verified that the critical load for uniaxial loading is always twice the critical load when loading is biaxial.

The results show that the element provides satisfactory results for practical use. Therefore, these elements can serve as a basis for other studies such as, analysis and optimization of plates using robust and efficient methods, such as genetic algorithms.

## V. ACKNOWLEDGEMENTS

The authors are grateful to the Civil Engineering Structures Group - GPEEC of the Federal University of Cariri - UFCA and for the financial support of CAPES, CNPQ and Funcap.

## VI. REFERENCES

[1] Arekar, V. A. e Bhavsar, B. B. Analytical Study of MERO Connector in Double Layer Grid Structure, 2(2), p. 35–42 2013.

[2] Makwski, Z. S. Estructuras espaciales de acero. 2o ed. Editorial Gustavo Gili, Barcelona. 1972.

[3] Bathe, K. J., (1996), Finite Element Procedures. Prentice-Hall.

[4] Belo, I. M., (2006), Análise Eficiente de Compósitos Laminados Planos utilizando-se a Formulação de Elementos Finitos corrigida a-priori sem os Efeitos do Travamento. Dissertação (Mestrado em Engenharia Mecânica), Pontifícia Universidade Católica do Paraná, Paraná.

[5] Cook, R. D., Malkus, D. S.; Plesha, M. E. E Witt, R. J., (2001), Concepts and Applications of Finite Element Analysis. 4th Edition, John Wiley & Sons.

[6] Crisfield, M. A., (1991), Non-linear Finite Element Analysis of Solids and Structures, vol. 1, John Wiley and Sons.

[7] Holanda, A. S., (2000), Análise do Equilíbrio e Estabilidade de placas com Restrições de Contato. Tese (Doutorado em Ciências em Engenharia Civil), Pontifícia Universidade Católica do Rio de Janeiro, Rio de Janeiro.

[8] Jones, R. M., (1999), Mechanics of Composite Materials. 2 ed. Philadelphia: Taylor & Francis.

[9] Martha, L. F.; Parente Jr., E. (2002), An Object-Oriented Framework for Finite Element Programming. Proceedings of Fifth World Congress on Computational Mechanics (WCCM V), Vienna: 2002, pp. 1–10.

[10] Reddy, J. N., (1996), Mechanics of Laminated Composite Plates – Theory and Analysis. New York: CRC Press.

[11] Vasiliev, V. V.; Morozov, E. V., (2001). Mechanics and Analysis of Composite Materials, Elsevier Science Ltd.

[12] Zienkiewicz, O. C.; Taylor, R. L., (2000), The Finite Element Method. 5ª ed. Butterworth-Heinemann.

## CITE AN ARTICLE

Da Silva, W., Sobrinho, B., Silva Freitas, C., Távora Ribeiro, B., De Morais Júnior, F., & Costa Silva, R. (2018). NUMERICAL ANALYSIS IN FINITE ELEMENTS OF LAMINATED PLATES IN STEEL APPLIED IN DIFFERENT TYPES OF COMPOSITE MATERIALS MODELED ABAQUS MODELING AND COMPARED WITH ANALYTICAL. *INTERNATIONAL JOURNAL OF ENGINEERING SCIENCES & RESEARCH TECHNOLOGY*, *7*(6), 531-551.